

Ferromagnetism in Mn-doped GaN: From clusters to crystals

G. P. Das,* B. K. Rao, and P. Jena

Physics Department, Virginia Commonwealth University Richmond, Virginia 23284-2000, USA

(Received 8 April 2003; published 15 July 2003)

The magnetic coupling between doped Mn atoms in clusters as well as crystals of GaN has been studied from first principles using molecular orbital theory for clusters and linearized muffin tin orbital—tight binding formulation for crystals. The calculations, based on density functional theory and the generalized gradient approximation for exchange and correlation, reveal the coupling to be ferromagnetic with a magnetic moment ranging from $2.0 \mu_B$ to $4.0 \mu_B$ per Mn atom depending on its environment. Mn atoms also tend to cluster and bind more strongly to N atoms than to Ga atoms. The significant binding of Mn to GaN clusters further indicates that it may be possible to increase the Mn concentration in GaN by using a porous substrate that offers substantial surface sites.

DOI: 10.1103/PhysRevB.68.035207

PACS number(s): 72.80.Ey, 75.30.Hx, 75.50.Pp

I. INTRODUCTION

The discovery of ferromagnetism in Mn-doped InAs and GaAs with a Curie point of 110 K^1 and the subsequent theoretical prediction² that the Curie point in Mn-doped GaN could be higher than the room temperature have created an intense interest in the study of dilute magnetic semiconductors (DMSs). Studies of these systems are driven not only by the academic interest in understanding the origin of ferromagnetism from a fundamental point of view but also by the fact that new semiconducting devices that combine electron's charge and spin could be of high technological interest.

There are two central questions that need to be addressed in the quest for doped magnetic semiconductors with a Curie temperature above 300 K : (i) What is the origin of the ferromagnetic coupling in these systems? (ii) How does one increase Mn concentration so that the magnetic ion density and consequently the Curie temperature (T_c) could be enhanced? Several attempts have been made in the recent years both experimentally and theoretically to address these issues. Overberg *et al.*³ reported a T_c between 10 and 25 K in GaN samples containing 7% Mn while Theodoropolou *et al.*⁴ and Reed *et al.*⁵ have reported ferromagnetism in (Ga,Mn)N with T_c of 250 and 228 – 370 K , respectively. Sonoda *et al.*⁶ succeeded in incorporating upto 9% Mn in GaN and estimated (by extrapolation of the magnetization vs temperature curve using mean field approximation) a T_c as high as 945 K . Although the growth mechanism seems to play a vital role, the reason for such a wide variation of T_c is not understood.

Recently Dhar *et al.*⁷ have measured the magnetic properties of (Ga,Mn)N layers grown on $4\text{H-SiC}(0001)$ by reactive molecular beam epitaxy by varying Mn/Ga flux ratio. They have found that the homogeneous alloy (Ga,Mn)N produced with low concentration of Mn exhibits anti-ferromagnetic Mn-Mn interaction and undergoes a spin glass transition at temperatures around 5 K . On the other hand, the sample of (Ga,Mn)N with 14% Mn exhibits ferromagnetic coupling with a Curie point of about 750 K . They have suggested that this ferromagnetism could originate from nm-scale Mn-rich clusters formed during the growth. This possibility was first proposed by Rao and Jena,⁸ who found clustering of Mn around N to be energetically favorable and

equally important is that the Mn atoms couple ferromagnetically leading to giant magnetic moments.

There have been several theoretical attempts based on model calculations to study this problem as well. The original explanation of ferromagnetism in DMS systems was given by Dietl *et al.*² in terms of hole-mediated Rudermann-Kittel-Kasuya-Yosida (RKKY) interaction. This approach, which implies that a Fermi surface must exist, has recently been questioned by Litvinov and Dugaev.⁹ These authors, instead, propose that ferromagnetism in DMS systems is due to localized spins in the magnetic impurity acceptor level of the semiconductor crystal, that excite band electrons due to s - p or p - d exchange interaction. Several first principles calculations^{8,10–12} have also been carried out to understand the magnetic properties of dilute magnetic semiconductors. Using local density supercell band calculations for $3d$ transition metal (TM)-doped III-V zinc-blende semiconductors, Schilfgaarde and Mrysov¹⁰ had shown that the anomalous exchange interactions between the impurity atoms deviate strongly from the RKKY-like simple models and undergo a transition from ferromagnetic (for Mn and Cr) to antiferromagnetic (for Fe) as a function of d -band filling. Sato and Katayama-Yoshida,¹¹ on the other hand, had carried out Korringa-Kohn-Rostoker coherent potential approximation (KKR-CPA) calculations in randomly substituted $3d$ TM impurities in GaN and found ferromagnetic state to be stable for half-filled or less than half-filled impurities such as Mn, Cr, and V. Both these first-principles investigations independently confirm that Mn atoms couple ferromagnetically in GaN. More recently Kronik *et al.*¹² used pseudopotential density functional calculations to investigate suitability of (Ga,Mn)N system for spin injection and transport.

In this paper we present the results of first principles theoretical calculations of the electronic structure, energetics, and magnetism of a Mn dimer-doped GaN in various structural forms that simulate binding of Mn on to surface as well as bulk sites. We investigate if Mn substitution is energetically favorable and if its binding energy depends on the environment. We also determine the charge and spin state of Mn and the coupling between the spins at Mn sites. We have done this by doping a pair of Mn atoms into $(\text{GaN})_x$ ($x \leq 3$) clusters (surface sites) as well as into wurtzite GaN crystal (bulk sites). This allows us to study if the coupling

between Mn atoms is ferromagnetic or antiferromagnetic. Since the environment around Mn sites changes significantly with cluster size as well as in the crystal, we are able to determine the effect of local bonding on the energetics, electronic structure, and magnetic properties of doped Mn. We find that the Mn atoms are coupled ferromagnetically irrespective of the hosts we have considered. This is particularly interesting since bulk Mn is antiferromagnetic while in very small clusters the coupling is ferromagnetic and/or ferrimagnetic.

In Sec. II we describe our theoretical procedure. The results are discussed in Sec. III and summarized in Sec. IV.

II. THEORETICAL PROCEDURE

The calculations on clusters were carried out by using the linear combination of atomic orbitals molecular orbital (LCAO-MO) method. The atomic orbitals centered at individual Ga, N, and Mn sites were represented by Gaussian orbitals. We used the frozen core LANL2DZ basis set available in the GAUSSIAN 98 code.¹³ The total energies were calculated using the density functional theory and generalized gradient approximation (GGA) for exchange and correlation.¹⁴ The geometries were optimized by calculating the force at every atomic site and relaxing the geometry until the forces vanish. The threshold for this was set at 0.000450 a.u./Bohr. Since Mn atom could carry a magnetic moment, the geometries were optimized for various spin multiplicities, $M=2S+1$ to arrive at the ground state.

In order to study the effect of the Mn impurity on the electronic structure of GaN crystal and the interaction between Mn magnetic moments, we have considered the hexagonal wurtzite structure which lies lower in energy than the cubic zincblende structure. A super cell which is eight times larger than the wurtzite GaN unit cell was constructed that accommodates 16 Ga and 16 N atoms. Two of the nearest Ga atoms were selectively replaced by Mn atoms so that the super cell formula unit becomes $Mn_2Ga_{14}N_{16}$. Recent experiment by Dhar *et al.*⁷ suggests that Mn atoms occupy substitutional sites. It should be noted, however, that this 32 atom super cell is one of the smallest super cell that ensures separation between the impurities in neighboring super cells by at least a few times the Ga-N bond length. Similar super cells have been used¹⁵ for a Be impurity in wurtzite GaN.

All the band structure calculations reported in this work have been performed using self-consistent tight-binding linear muffin-tin orbital (TB-LMTO) method with the atomic sphere approximation and the ‘‘combined correction.’’¹⁶ We have used the density functional theory and generalized gradient approximation for exchange-correlation as per the original Perdew-Wang formulation.¹⁷ The super cell is divided into space-filling and therefore slightly overlapping spheres centered on each atom. Since the wurtzite GaN is an open structure, we had to introduce two different types of empty spheres (two of each type) in the unit cell of GaN, thereby making the total number of spheres in the wurtzite unit cell as 8. This translates to a 64-atom supercell with 32 real atoms and 32 empty spheres. All the calculations have been performed with the experimental lattice parameters (a

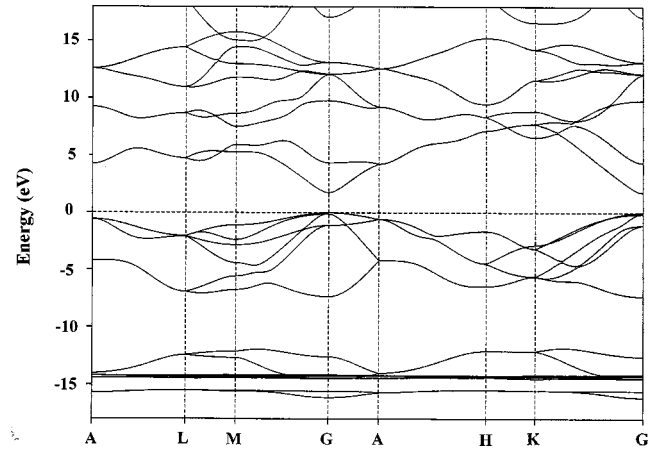


FIG. 1. Band structure of wurtzite GaN.

$=3.189 \text{ \AA}$ and $c=5.185 \text{ \AA}$). When Mn goes into a Ga-substitutional position, there is a strong Mn-N bonding resulting in formation of stable Mn_2N clusters on which independent cluster calculations have been performed. We have neglected any structural relaxation effect in the first shell N neighbors of Mn (subsequent shells are anyway expected to be unperturbed). This is based upon the recent cluster calculation⁸ where Mn-N distance was seen to vary with Mn concentration ranging from 1.62 \AA in the MnN dimer to 1.96 \AA in the Mn_5N cluster. We will show in this paper that Mn-N distances in $(GaN)_xMn_2$ clusters also vary from 1.78 \AA in $(GaN)Mn_2$ to 1.92 \AA in $(GaN)_3Mn_2$ clusters. The distance between Ga and N in bulk GaN is 1.96 \AA . Thus, we do not expect significant relaxation in the Mn-N distance in bulk GaN. More importantly, Wang *et al.*¹⁸ have calculated the total energies and magnetic properties of $(Ga,Mn)N$ using a $GaN(11\bar{2}0)$ slab and replacing two Ga atoms by two Mn atoms at successive locations. They allowed the two top layers to relax. They have found the magnetic moment and coupling of Mn atoms to remain unchanged due to relaxation.

Using the so-called Hartree potential plot prescription, we have fixed the Ga and N atomic sphere radii to be 1.227 and 1.015 \AA , which are roughly proportional to the corresponding covalent radii of 1.62 and 1.26 \AA of Ga and N, respectively. For Mn atomic spheres, we have used the same atomic sphere radius as that of Ga. Brillouin zone (BZ) integration has been performed using the improved tetrahedron method.¹⁹ In all our supercell calculations, we have used $(6,6,4)$ \mathbf{k} mesh which corresponds to 84 \mathbf{k} points in the irreducible wedge of the simple cubic BZ. Spin-polarized scalar relativistic (i.e., without spin-orbit interaction which is not significant for GaN) calculations have been performed with minimal basis set consisting of s , p , and d orbitals ($\ell=2$) for Ga, Mn, and N, with N- d orbitals downfolded. Note that the localized semicore $3d$ states of Ga have been treated as fully relaxed band states, as emphasized by other workers^{15,19} also. Apart from the valence states of Ga, Mn, and N, the core orbitals were kept frozen to their isolated atomic form.

We have first benchmarked our calculations by comparing the electronic, cohesive and structural properties of bulk Wurtzite GaN with those reported in the literature. The band structure in Fig. 2 shows a direct gap of ≈ 2 eV at the

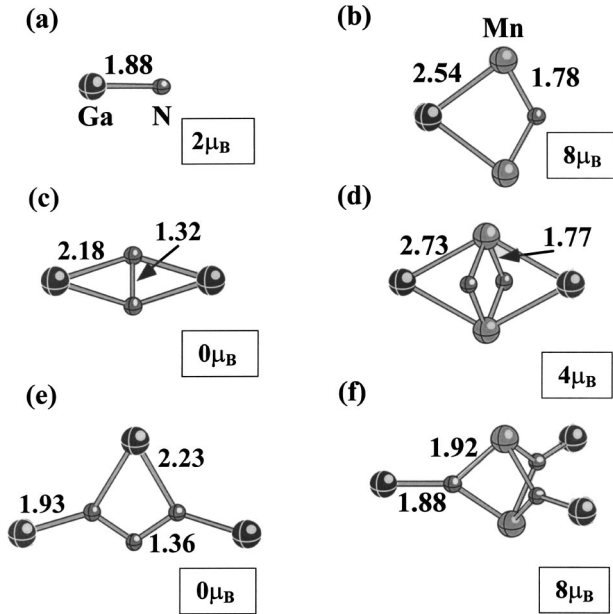


FIG. 2. Ground state cluster geometries of $(\text{GaN})_x$ (left panel) and $(\text{GaN})_x\text{Mn}_2$ (right panel). The magnetic moment of each cluster is also provided.

Γ -point, which can be artificially ‘opened up’ to match with the experimental gap, by applying some external ℓ -dependent potential (as done by Christensen and Gorczyca²⁰ for calculating deformation potential and the optical properties etc.) The zero of the energy is fixed at the top of the valence band, which consists of s - and p -orbitals of Ga and N. The semicorelike $3d$ states appear as narrow bands ~ 10 eV below the Fermi level. The valence bandwidths $W1$, $W2$, and $W3$ are found to be 7.2, 2.6, and 0.7 eV, respectively, which are in very good agreement with the orthogo-

nalized LCAO results²¹ on Wurtzite GaN. Since the overestimation of the binding energy and the underestimation of the band gap are typical of local density approximation that are partially salvaged by incorporation of GGAs, we have used GGAs as discussed above in all our calculations. More rigorous (and also computationally demanding) GW calculations have been reported²² that show improved energy gaps due to incorporation of nonlocal exchange-correlation potential.

III. RESULTS

We first discuss the results of magnetic coupling between Mn atoms doped into $(\text{GaN})_x$ clusters and compare that with the bulk result. As indicated before, the environment of Mn in $(\text{GaN})_x$ clusters where most atoms are on the surface versus that in the bulk can illustrate how sensitive the magnetic coupling and the magnitude of the magnetic moment are to interatomic separation and atomic coordination.

A. Mn_2 doped $(\text{GaN})_x$ ($x \leq 3$) clusters

It is *a priori* not clear what is the magnetic coupling (ferromagnetic versus anti-ferromagnetic) between Mn atoms and the total magnetic moment of the $\text{Mn}_2(\text{GaN})_x$ clusters. Thus we have carried out geometry optimization for all possible spin multiplicities, $M = 2S + 1$. The total magnetic moment of the cluster is then $M - 1$. The ground state geometries along with the corresponding magnetic moments are given in Fig. 2. The geometries for other spin configurations are similar to those in Fig. 2. In Table I we provide information on the Mn-Mn distance in $\text{Mn}_2(\text{GaN})_x$ ($x \leq 3$) clusters for different spin multiplicities. Also listed in the table are the magnetic moment at the Ga, N, and Mn sites and the relative energies measured with respect to the ground state spin multiplicity.

TABLE I. Distribution of magnetic moments and Mn-Mn distance in $\text{Mn}_2(\text{GaN})_x$ ($x \leq 3$) clusters as a function of spin multiplicity, $M = 2S + 1$. The energy ΔE for each spin multiplicity is given with respect to the ground state structure.

Cluster	Multiplicity	ΔE (eV)	Spin (μ_B) at the site of			Mn-Mn distance (\AA)
			Ga	N	Mn	
$\text{Mn}_2(\text{GaN})$	3	2.33	0.06	-0.02	0.98	3.23
	5	1.46	-0.37	-0.36	2.37	3.19
	7	0.69	-0.16	-0.30	3.23	3.01
	9	0.0	-0.13	-0.06	4.10	3.11
	11	0.34	0.62	0.06	4.66	3.05
$\text{Mn}_2(\text{GaN})_2$	3	1.09	-0.32	-0.01	1.33	2.56
	5	0.0	-0.09	0.06	2.03	2.52
	7	0.51	0.11	0.06	2.83	2.71
	9	2.37	0.82	0.13	3.05	2.84
$\text{Mn}_2(\text{GaN})_3$	5	1.56	0.19, -0.02	0.19, 0.13	1.60	2.48
	7	0.98	0.25, -0.20	-0.16, -0.07	3.00	2.72
	9	0.0	0.09, 0.01	0.36, 0.32	3.44	2.44
	11	1.39	0.06, 0.07	-0.10, -0.02	5.04	3.52

TABLE II. Energetics of $(\text{GaN})_x$ and $(\text{GaN})_x\text{Mn}_2$ complexes. See Eqs. (1)–(3) for definitions.

x	E_b (eV)	ΔE (eV)	ΔE_0 (eV)
1	0	5.39	-
2	2.99	3.73	5.97
3	3.33	4.34	4.03

We first discuss the equilibrium geometries of $\text{Mn}_2(\text{GaN})_x$ clusters corresponding to the most preferred spin configuration with those of $(\text{GaN})_x$ clusters in Fig. 2. Some of the representative bond distances are marked in the figure. The Ga-N distance in the dimer is 1.88 Å and changes only slightly as clusters grow. Note that the nearest distance between Ga and N in the wurtzite crystalline GaN is 1.95 Å. These close values between inter-atomic distances in clusters and crystals is characteristic of covalently bonded systems. As the $(\text{GaN})_x$ clusters are doped with Mn atoms, the structures change significantly. The GaN bond distances get enlarged by almost 1 Å in going from GaN to $(\text{GaN})\text{Mn}_2$, but this enhancement decreases rapidly in larger $(\text{GaN})_x\text{Mn}_2$ clusters yielding a value of about 2.73 Å in $(\text{GaN})_2\text{Mn}_2$ and 1.88 Å in $(\text{GaN})_3\text{Mn}_2$. Since this GaN bond distance is close to that in GaN crystal, namely, 1.95 Å, it indicates that doping of Mn into clusters may illustrate the salient features of the electronic structure of bulk Mn-doped GaN. We also note from Table I that Mn-Mn distances in $(\text{GaN})_x\text{Mn}_2$ clusters vary from 3.11 Å in $(\text{GaN})\text{Mn}_2$ to 2.44 Å in $(\text{GaN})_3\text{Mn}_2$. In bulk α -Mn, the Mn-Mn distances also vary over a wide range, namely, between 2.25 and 2.95 Å.

We now discuss the energetics of these clusters. The binding energy of $(\text{GaN})_x$ clusters is defined as

$$E_b = [xE(\text{GaN}) - E(\text{GaN})_x]/x. \quad (1)$$

We define the energy gain in adding a GaN dimer to an existing $(\text{GaN})_{x-1}$ cluster as

$$\Delta E_0 = E(\text{GaN}) + E[(\text{GaN})_{x-1}] - E[(\text{GaN})_x]. \quad (2)$$

Similarly, the energy gain in adding two Mn atoms to an existing $(\text{GaN})_x$ cluster is defined as

$$\Delta E = E[(\text{GaN})_x] + 2E(\text{Mn}) - E[(\text{GaN})_x\text{Mn}_2]. \quad (3)$$

Here E represents the total energy of the corresponding systems. The results are given in Table II. We first note that the binding energy of a GaN dimer measured against dissociation into Ga and N atoms is 2.18 eV. As associative GaN units are added, the binding energy in Eq. (1) steadily increases. On the other hand, the energy gain in adding successive GaN units [see Eq. (2)] first increases and then decreases, indicating that $(\text{GaN})_2$ is a relatively more stable unit.

Doping of Mn atoms to $(\text{GaN})_x$ clusters is found to be energetically quite favorable. For example, the addition of two Mn atoms to a GaN dimer results in an energy gain of 5.39 eV. It should be mentioned that the binding energy of a Mn_2 dimer is less than 0.1 eV as the Mn atom has a half-filled $3d$ shell and a filled $4s$ shell, and hence interacts

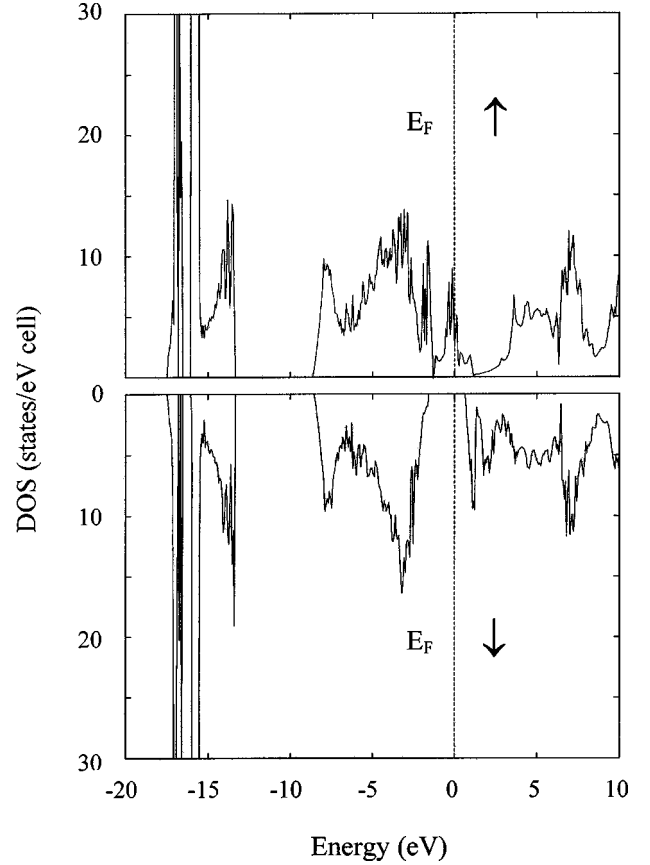


FIG. 3. Total density of states of a wurtzite $(\text{Ga}_{14}\text{Mn}_2)\text{N}_{16}$ supercell for majority spin (top) and minority spin (bottom).

weakly with another Mn atom. The nature of bonding changes in the presence of GaN. Mn and N atoms form a strong bond due to charge transfer from Mn to N. As a matter of fact, the binding energy of MnN dimer is 3.07 eV which is significantly larger than that of GaN, namely, 2.18 eV. In addition, the two Mn atoms that interact weakly with each other in Mn_2 due to their closed $4s$ shells, no longer do so in the presence of N. Their coupling is mediated by N. The fact that the bonding of MnN is stronger than that of GaN suggests that when Mn is deposited on the GaN substrate, Mn can replace Ga atoms and cluster around N. This is confirmed by recent experiment of Prokes and co-workers.²³ Since small $(\text{GaN})_x$ clusters represent all surface atoms, our results suggest that the doping of Mn in GaN surfaces as well as porous GaN that contains large surface area is energetically favorable. The successive energy gains in adding two Mn atoms to $(\text{GaN})_x$ clusters are also substantial although they tend to oscillate with cluster size.

We now consider the magnetic properties of these clusters. In Fig. 2 we list the total magnetic moments of the clusters for which the energy is the minimum. The magnetic moments of free Ga, N, and Mn atoms are, respectively, $1\mu_B$, $3\mu_B$, and $5\mu_B$. The magnetic moments of clusters of $(\text{GaN})_x$ are $2\mu_B$ for $x=1$ and $0\mu_B$ for $x=2$ and 3. For those clusters that have finite magnetic moment, much of it is located at the N site which is antiferromagnetically coupled to the moment at the Ga site. As clusters increase in size, it is

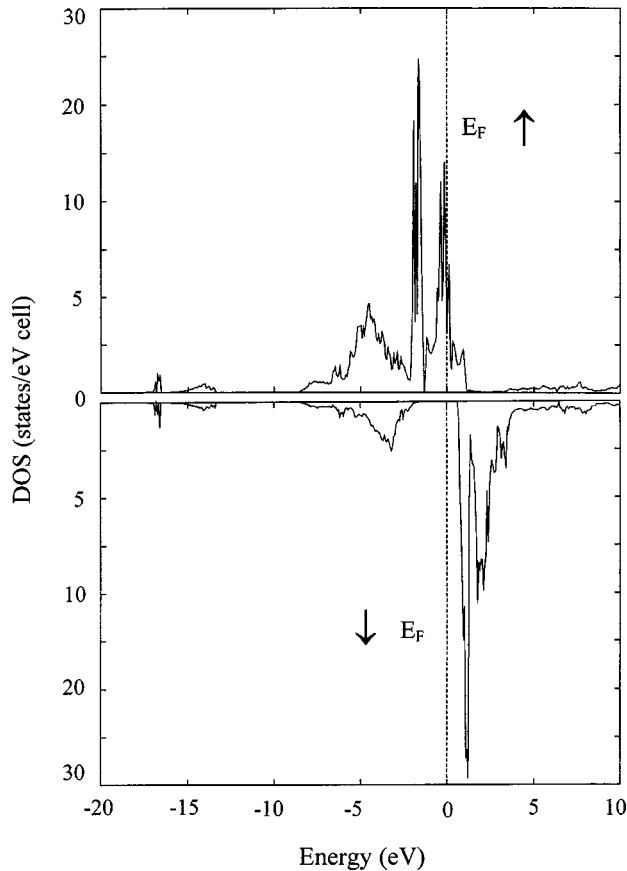


FIG. 4. Partial density of states of a wurtzite $(\text{Ga}_{14}\text{Mn}_2)\text{N}_{16}$ supercell projected onto a Mn site, for majority spin (top) and minority spin (bottom).

expected that the individual moments at Ga and N sites will decrease and eventually vanish since bulk GaN is nonmagnetic. We already see this happen in clusters as small as $(\text{GaN})_3$.

As the Mn atoms are doped, the $(\text{GaN})_x\text{Mn}_2$ ($x \leq 3$) clusters exhibit substantial magnetic moments. For example, the total magnetic moments of $(\text{GaN})\text{Mn}_2$ and $(\text{GaN})_3\text{Mn}_2$ are $8\mu_B$ each. Most of these moments are localized at the Mn sites (Table I), and the two Mn atoms are coupled ferromagnetically. The moments at Ga and N sites are very small and couple mostly antiferromagnetically to those at Mn sites. In most of these clusters the Mn-Mn distance is larger than 2.5 Å. It has been known from studies of free Mn (Ref. 24) and MnO (Ref. 25) clusters that the coupling between Mn atoms could be antiferromagnetic if their inter-atomic distances are reduced. Thus, it is important that for Mn atoms to couple ferromagnetically, they need to be kept apart by more than 2.5 Å. In bulk GaN this is not a problem as Mn's substituted for the Ga site and the nearest neighbor distance between two Ga atoms in bulk GaN is 3.19 Å. We will show in the following through LMTO-TB band structure calculations that this is indeed the case.

B. Mn_2 doped in wurtzite GaN crystal

For our bulk calculations, we have used a pair of Mn atoms replacing Ga sites in the wurtzite GaN bulk crystal.

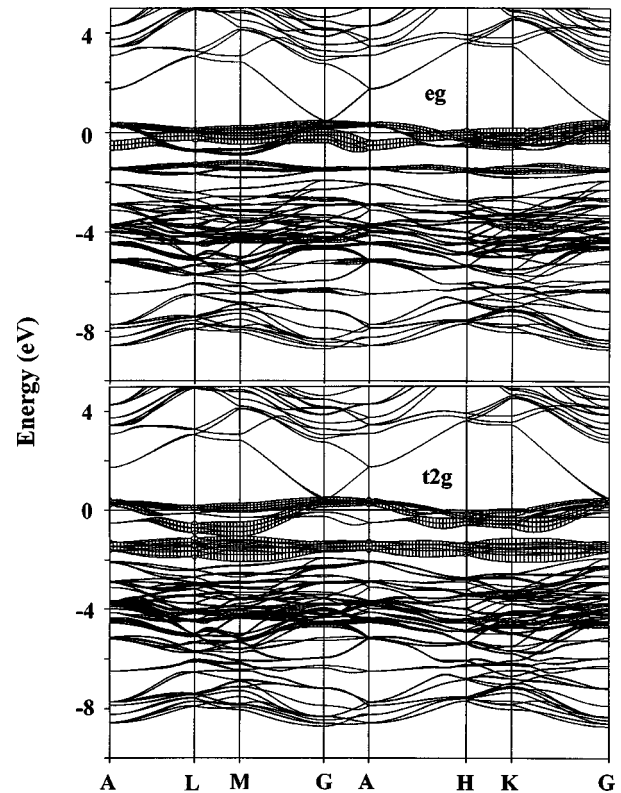


FIG. 5. Energy band structure of $\text{Ga}_{14}\text{Mn}_2\text{N}_{16}$ (majority spin) along selected high symmetry directions. The fat-bands are projections on to Mn- e_g (top) and Mn- t_{2g} (bottom); see the text for details.

The reason why we used Mn dimer, rather than a single Mn impurity atom is that we are interested to see if the coupling between Mn spins is ferromagnetic coupling and to compare it with our cluster results. Accordingly our supercell, as mentioned in Sec. II has the formula unit $\text{Mn}_2\text{Ga}_{14}\text{N}_{16}$, and the Mn-Mn distance we have chosen is 3.19 Å. This distance is more than the critical distance of 2.5 Å obtained above from our cluster calculations. The results of our supercell band calculations reported here are all for ferromagnetic configuration, which is favored over antiferromagnetic configuration for Mn-doped GaN.^{10,11} This is also supported by total energy considerations. The total and partial (Mn-projected) densities of states (DOS) of $\text{Mn}_2\text{Ga}_{14}\text{N}_{16}$ (Figs. 3 and 4) show that the Fermi level passes through Mn d bands for the majority spin. The minority spin Mn d band lies above the Fermi level and merges with the bottom of the conduction band, within the expected local density approximation (LDA) bandgap. This confirms the half-metallic nature of this system, although both majority and minority spin DOSs show a common gap. The paramagnetic DOS (i.e., without spin-polarization) shows a ~ 2.4 eV wide Mn $3d$ band hybridized with Mn $2p$. The t_{2g} level lies above the e_g level thereby indicating that Mn is sitting in tetrahedral, rather than octahedral crystal field environment in the GaN lattice. This is in conformity with the results obtained by Schilf-garde and Mryasov¹⁰ and by Sato and Katayama-Yoshida.¹¹ When spin polarization is switched on, there is a further spin-splitting by as much as ~ 2 eV. The peak of the majority

spin Mn d band lies ~ 1.8 eV above the top of the valence band of GaN. This conforms to the conventional wisdom of Mn acting as an effective mass acceptor (d^5+h) and also with the recent deep-level optical spectroscopy measurements on lightly Mn-doped samples,²⁶ which indicates that Mn forms a deep acceptor level at 1.4 eV above the GaN band gap. The dispersions of the e_g and t_{2g} bands in the hexagonal plane (i.e., perpendicular to the c axis) are clearly seen from the projected fat-bands of the respective Mn orbitals (Fig. 5). Each of the fat band has been allocated a width proportional to the (sum of the) weight(s) of the corresponding orthonormal orbital(s). The minimum gap (direct) appears at the M point. What is important is that the Fermi level passes right through the fattened impurity band (majority-spin), thereby confirming that the impurity level acts as an effective mass acceptor.

Our supercell calculations yield a localized magnetic moment of $\sim 3.5\mu_B$ manifested on the Mn atom. Some weak polarization is also observed to be induced onto the nearest neighbor N atoms in the host semiconductor lattice surrounding the magnetic impurity atom. This is in agreement with the results reported by Fong *et al.*²⁷ and by Schilfgaard and Mrysov¹⁰ from their LDA supercell calculations on zincblende GaN doped with Mn. The latter investigators argued about the possible formation of small Mn clusters in GaN, and also how the ferromagnetic coupling strength is expected to decrease with Mn concentration going either way from some critical concentration. Our calculations also

indicate the ferromagnetic coupling to decrease and even vanish with increasing Mn-Mn separation and for a Mn impurity going to an interstitial rather than a Ga-substitutional position in the wurtzite lattice.

IV. SUMMARY

The above results indicate that the coupling between Mn atoms is ferromagnetic whether they are doped into the crystal or clusters. Equally interesting is our finding that the Mn atoms retain a magnetic moment of about $3.5\mu_B$ irrespective of their environment. Since clusters represent an extreme case of surface states and crystal sites represent a substitutional bulk environment, we are convinced that doping of Mn in GaN whether they are porous, crystalline, or thin layers would lead to ferromagnetic coupling between Mn atoms. Our results further suggest that clustering of Mn around N is energetically favorable. The sensitivity of the measured T_c 's to experimental growth conditions may very well be due to the clustering of Mn around N.

ACKNOWLEDGMENTS

This work was supported by a grant from the Office of Naval Research under a Defense University Research Initiative on Nanotechnology (DURINT). B.K.R. and P.J. also acknowledge support from the Department of Energy (DE-FG02-96ER45579).

*On leave from Bhabha Atomic Research Center, Mumbai, India.

¹H. Ohno, *Science* **281**, 951 (1998).

²T. Dietl, H. Ohno, F. Matsukura, J. Cibert, and D. Ferrand, *Science* **287**, 1019 (2000); T. Dietl, H. Ohno, and F. Matsukura, *Phys. Rev. B* **63**, 195205 (2001); T. Dietl, F. Matsukura, and H. Ohno, cond-mat/0109245 (unpublished).

³M. E. Overberg, C. R. Abernathy, S. J. Pearton, N. A. Theodoropoulou, K. T. McCarthy, and A. F. Hebard, *Appl. Phys. Lett.* **79**, 1312 (2001).

⁴N. Theodoropoulou, A. F. Hebard, M. E. Overberg, C. R. Abernathy, S. J. Pearton, S. N. G. Chu, and R. G. Wilson, *Appl. Phys. Lett.* **78**, 3475 (2001).

⁵M. L. Reed, N. A. El-Masry, H. H. Stadelmaier, M. K. Ritums, M. J. Reed, C. A. Parker, and S. M. Bedair, *Appl. Phys. Lett.* **79**, 3473 (2001).

⁶S. Sonada, S. Shimizu, T. Sasaki, Y. Yamamoto, and H. Hori, cond-mat/0108159 (unpublished).

⁷S. Dhar, O. Brandt, A. Tampert, L. Däweritz, K. J. Friedland, K. H. Plogg, J. Kaller, B. Beschoten, and G. Gäntherodt, *Appl. Phys. Lett.* **82**, 2077 (2003).

⁸B. K. Rao and P. Jena, *Phys. Rev. Lett.* **89**, 185504 (2002).

⁹V. I. Litinov and V. K. Dugaev, *Phys. Rev. Lett.* **86**, 5593 (2001).

¹⁰M. van Schilfgaard and O. N. Mryasov, *Phys. Rev. B* **63**, 233205 (2001).

¹¹K. Sato and H. Katayama-Yoshida, *Jpn. J. Appl. Phys.* **40**, L485 (2001); *Semicond. Sci. Technol.* **17**, 367 (2002).

¹²L. Kronik, M. Jain, and J. R. Chelikowsky, *Phys. Rev. B* **66**, 041203(R) (2002).

¹³GAUSSIAN 98, Revision A.7, M. J. Frisch, G. W. Trucks, H. B.

Schlegel, G. E. Scuseria, M. A. Robb, J. R. Cheeseman, V. G. Zakrzewski, J. A. Montgomery, Jr., R. E. Stratmann, J. C. Burant, S. Dapprich, J. M. Millam, A. D. Daniels, K. N. Kudin, M. C. Strain, O. Farkas, J. Tomasi, V. Barone, M. Cossi, R. Cammi, B. Mennucci, C. Pomelli, C. Adamo, S. Clifford, J. Ochterski, G. A. Petersson, P. Y. Ayala, Q. Cui, K. Morokuma, D. K. Malick, A. D. Rabuck, K. Raghavachari, J. B. Foresman, J. Cioslowski, J. V. Ortiz, A. G. Baboul, B. B. Stefanov, G. Liu, A. Liashenko, P. Piskorz, I. Komaromi, R. Gomperts, R. L. Martin, D. J. Fox, T. Keith, M. A. Al-Laham, C. Y. Peng, A. Nanayakkara, C. Gonzalez, M. Challacombe, P. M. W. Gill, B. Johnson, W. Chen, M. W. Wong, J. L. Andres, C. Gonzalez, M. Head-Gordon, E. S. Replogle, and J. A. Pople, Gaussian, Inc., Pittsburgh PA, 1998.

¹⁴A. D. Becke, *Phys. Rev. A* **38**, 3098 (1988); J. P. Perdew, K. Burke, and Y. Wang, *Phys. Rev. B* **54**, 16 533 (1996); K. Burke, J. P. Perdew, and Y. Wang, in *Electronic Density Functional Theory: Recent Progress and New Directions*, edited by J. F. Dobson, G. Vignale, and M. P. Das (Plenum, New York, 1998).

¹⁵C. G. van de Walle, S. Limpijumngong, and J. Neugebauer, *Phys. Rev. B* **63**, 245205 (2001).

¹⁶O. K. Andersen, *Phys. Rev. B* **12**, 3060 (1975); O. K. Andersen, and O. Jepsen, *Phys. Rev. Lett.* **53**, 2571 (1984). We have used the latest version of the Stuttgart TB-LMTO-ASA program.

¹⁷J. P. Perdew and Y. Wang, *Phys. Rev. B* **33**, 8800 (1986); J. P. Perdew, *ibid.* **33**, 8822 (1986); J. P. Perdew and Y. Wang, *ibid.* **45**, 13 244 (1992).

¹⁸Q. Wang, Q. Sun, B. K. Rao, and P. Jena (unpublished).

- ¹⁹P. Bloechl, O. Jepsen, and O. K. Andersen, *Phys. Rev. B* **49**, 16 223 (1994).
- ²⁰N. E. Christensen and I. Gorczyca, *Phys. Rev. B* **50**, 4397 (1994).
- ²¹Y.-N. Xu and W. Y. Ching, *Phys. Rev. B* **48**, 4335 (1993).
- ²²M. van Schilfgaarde and O. Mryasov, in *Proc. of APS Meeting, Minneapolis, MN 2000, Abstract, Vol. 26*; *Phys. Rev. B* **63**, 233205 (2001).
- ²³S. Prokes (private communication).
- ²⁴S. K. Nayak, M. Nooijen, and P. Jena, *J. Phys. Chem. A* **103**, 9853 (1999); S. N. Khanna, B. K. Rao, P. Jena, and M. Knickelbein, *Chem. Phys. Lett.* (to be published).
- ²⁵S. K. Nayak and P. Jena, *J. Am. Chem. Soc.* **121**, 644 (1999).
- ²⁶R. Y. Korotkov, J. M. Gregie, and B. W. Wessels, *Appl. Phys. Lett.* **80**, 1731 (2002).
- ²⁷C. Y. Fong, V. A. Gubanov, and C. Boekema, *J. Electron. Mater.* **29**, 1067 (2000).